Biochemical and Biophysical Research Communications **271,** 244–249 (2000)
doi:10.1006/bbrc.2000.2603, available online at http://www.idealibrary.com on IDEAL®

ADP Modulates the Dynamic Behavior of the Glycolytic Pathway of *Escherichia coli*

Juan C. Diaz Ricci

Departamento de Bioquímica de la Nutrición, Instituto Superior de Investigaciones Biológicas (CONICET-UNT), Instituto de Química Biológica "Dr. Bernabé Bloj," Facultad de Bioquímica, Química y Farmacia, Universidad Nacional de Tucumán, Chacabuco 461, 4000 Tucumán, Argentina

Received March 28, 2000

A mathematical model that includes biochemical interactions among the PTS system, phosphofructokinase (PFK), and pyruvate kinase (PK) is used to evaluate the dynamic behavior of the glycolytic pathway of *Escherichia coli* under steady-state conditions. The influence of ADP, phosphoenolpyruvate (PEP), and fructose-6-phosphate (F6P) on the dynamic regulation of this pathway is also analyzed. The model shows that the dynamic behavior of the system is affected significantly depending on whether ADP, PEP, or F6P is considered constant a steady state. Sustained oscillations are observed only when dADP/dt ≠ 0 and completely suppressed if dADP/dt = 0 at any steady-state value. However, when PEP or F6P is constant, the system evolves toward the formation of stable limit cycles with periods ranging from 0.2 min to hours.

***Key Words: Escherichia coli;* glycolytic pathway; dynamic behavior; oscillations.**

The dynamic behavior of the glycolytic pathway has intensively been studied because it presents a broad range of complex and interesting interactions among enzymes and their regulatory metabolites. Previous studies carried out with mathematical models revealed an amazing variety of dynamic modes when the system was perturbed in different manners (1–7) or imposed different schemes of regulation (8–12). However, in most of those studies kinetic expressions or metabolic pathways that were not specific of *Escherichia coli* have been used, hence, it is difficult to get a clear idea about the influence of specific enzymatic effectors or regulatory loops on the dynamic behavior of the glycolytic pathway of *E. coli*.

In the present study, a simplified mathematical model was designed preserving the most significant biochemical components involved in the regulation of the glucose metabolism of *E. coli*. The model was used to analyze the behavior of the high- and central-segment of the glycolytic pathway and to explore the dynamic regulatory pattern of the most controlling enzymatic steps involved—e.g., the phosphotransferase system (PTS), phosphofructokinase (PFK) and pyruvate kinase (PK)—under steady state conditions (13). Also, the temporal evolution of ATP, ADP, phosphoenolpyruvate (PEP) and fructose-6-phosphate (F6P) under different conditions was studied.

The mechanism of glucose uptake was included in the model, because this transport process, carried out by the PTS system, has rarely been included in previous studies and represents the most important mechanism of glucose uptake in *E. coli* (14, 15). The influence of PEP on the regulation of the pathway was included in this analysis, because this sole metabolite directly regulates not only the PTS system (16, 17) but the enzymes PFK (18, 19) and PK (20, 21) as well. I was particularly interested to study the behavior of the glycolytic pathway of *E. coli* because it has a phosphofructokinase that is not allosterically regulated by ATP or fructose-1,6-diphosphate (FDP) as it was usually assumed in other systems (4, 22), but by ADP and PEP (6, 18, 19), and this metabolic scenario has not yet been explored.

The model is also used to test the hypothesis that intermediate metabolites involved in the regulation of the pathway (e.g., ATP, ADP, PEP and F6P) can reach at a stable steady state (or pseudo-steady state) during balanced cell growth (23) or in resting cells, as it was assumed in earlier reports (24–27). Consequently, with the aim to evaluate the influence of these metabolites in the global regulation of the pathways, the model was studied under conditions that are normally assumed in experimental work. The analysis was focused on the evolution of ADP, PEP and F6P during glucose consumption under steady state conditions, not at a constant glucose input rate (5–7, 10, 28), but being regulated by the PTS loop that incorporates a new regulatory condition to this study. Experimental evi-

0006-291X/00 $35.00

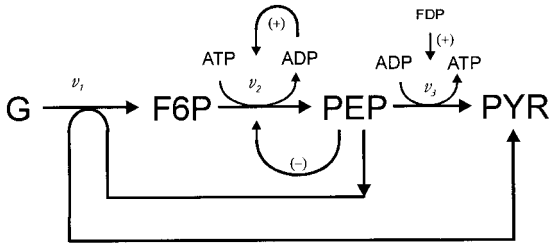

FIG. 1. Simplified metabolic pathway considered in the model. The scheme includes all regulatory effects exerted by the metabolites included in this study. Abbreviations: G, glucose; F6P, fructose-6-phosphate; FDP, fructose-1,6-diphosphate; PEP, phosphoenolpyruvate and PYR, pyruvate.

dence shows that when glucose is added to a suspension of resting cell of *E. coli*, the concentration of ADP decreases and F6P increases (27) (unfortunately no information is provided for PEP). Therefore, if ADP were required for the activation of PFK (18), glucose consumption would induce the partial inactivation of the enzyme due to the formation of ATP (29), but that was not observed experimentally. On the other hand, if glucose transport consumes PEP (14, 17) and PEP inhibits the PFK (18, 19), the glucose transport and the carbon flux through the pathway would be seriously affected by the evolution of PEP during glucose metabolism. This physiological situation opens interesting questions about the role of ADP and PEP on the regulation of carbon flux through this pathway. From technological point of view, the regulatory pattern involved in this pathway deserves special attention, because, although *E. coli* is the most important organism used in biotechnology, its intimate metabolic regulation remains almost unknown.

For the sake of clarity and to simplify the analysis of results, the model was studied considering constant ATP/ADP, F6P or PEP (one at a time), keeping constant and at physiologically levels the other kinetic parameters (29). The biological significance of the observed regulatory patterns is discussed.

MODEL DESCRIPTION

The model is based on flux balances of the intermediate metabolites (Fig. 1) and includes three enzymatic steps: PTS system, PFK and PK (Eqs. [1]–[4]). Simplification criteria were based on the analysis of the most controlling steps in this pathway (13, 14, 30–33). The present model resembles a model proposed by Markus and Hess (6), except that the source of glucose (G) was considered constant, and the substrate input rate (v_1) was allow to be self-regulated through the PTS system, hence, affected only by the intracellular availability of PEP.

PTS system consists in a complex of four proteins that transfer a phosphate group in a cascade reaction from PEP to PTS carbohydrate (14). Although each of the enzymatic steps of the phosphorylation cascade is reversible (16), the overall reaction is considered irreversible under physiological conditions. The reaction shows a Michaelis–Menten double substrate kinetics with K_m for glucose and PEP equal to 0.01 and 0.11 mM, respectively (15, 16, 34). The value of K_m for glucose permits the first simplification of the model when fixing a high and constant glucose concentration (i.e., 50 mM). Since [G] $\gg K_m$ for glucose (0.01 mM), the double substrate kinetics (34) reduces to a single substrate kinetics displaying a PEP-dependent glucose uptake (Eq. [5]).

PFK is an allosteric tetrameric enzyme that catalyzes the irreversible phosphorylation of fructose-6-phosphate (F6P) to fructose 1,6-diphosphate (FDP) using ATP as the phosphate donor. The PFK of *E. coli* shows homotropic cooperative interaction with respect to F6P, heterotropic allosteric activation by ADP and heterotropic allosteric inhibition by PEP (18). According to the concerted transition theory (35), PFK allosteric kinetics of *E. coli* depends on the allosteric equilibrium coefficient (L), which also depends on the simultaneous effect of the activator (ADP) and the inhibitor (PEP) (18).

PK is another allosteric tetrameric enzyme that catalyzes the irreversible phosphorylation of ADP from PEP rendering ATP and pyruvic acid (PYR) (Fig. 1). It has been shown that FDP has a strong activation effect on PK but only when the concentration of FDP is below 5 mM (20, 21). For that reason, the intracellular concentration of FDP was fixed at 5 mM which is an acceptable physiological value (27) and would keep PK completely activated. The PK kinetics also depends on the concentration of Mg^{2+} and K^+, therefore, the intracellular concentration of these cations were fixed high enough (see below) to keep the enzyme fully activated and to make the kinetics Mg^{2+} and K^+ independent (6, 20, 21). Since glycolytic enzymatic steps comprised from FDP to PEP present fast equilibrium kinetics (29, 30) they were lumped in a single step as shown in Fig. 1.

The system depicted in Fig. 1 can be described by the following set of differential equations where

$$\frac{dADP}{dt} = \nu_2 - \nu_3 \qquad [1]$$

$$\frac{dF6P}{dt} = \nu_1 - \nu_2 \qquad [2]$$

$$\frac{dPEP}{dt} = 2\nu_2 - \nu_1 - \nu_3 \qquad [3]$$

$$\frac{dATP}{dt} = \nu_3 - \nu_2, \qquad [4]$$

$$v = \sigma_1 \cdot \phi_1;\ v_2 = \sigma_2 \cdot \phi_2;\ v_3 = \sigma_3 \cdot \phi_3.$$

σ_i: maximum reaction rate; ϕ_i: saturation function of PTS system, PFK and PK enzymes (18, 20, 21, 34) defined as:

$$\phi_1 = \frac{\beta_1}{1 + \beta_1} \quad [5]$$

$$\phi_2 = \frac{\alpha\delta R^{n-1} + L c_\alpha c_\delta \alpha\delta T^{n-1}}{R^n + L T^n} \quad [6]$$

$$\phi_3 = \frac{\beta_3\gamma_2\mu}{1 + \beta_3 + \gamma_2 + \beta_3\gamma_2\mu} \quad [7]$$

with

$$L = L_0 \frac{(1 + c_\beta\beta_2)^n (1 + c_\gamma\gamma_1)^n}{(1 + \gamma_1)^n} \quad [8]$$

$$R = 1 + \alpha + \delta + \alpha\delta \quad [9]$$

$$T = 1 + \alpha c_\alpha + \delta c_\delta + \alpha\delta \cdot c_\alpha c_\delta \quad [10]$$

In these expressions α (F6P/$K_{2R(F6P)}$), β_1 (PEP/K_{1PEP}), β_2 (PEP/$K_{2R(PEP)}$), β_3 (PEP/K_{3B1}), γ_1 (ADP/$K_{2R(ADP)}$), γ_2 (ADP/K_{3A1}), δ (ATP/$K_{2R(ATP)}$) and μ (Mg^{2+}/K_{3F1}) denote normalized concentrations (dimensionless) of F6P, PEP, ADP, ATP and Mg^{2+}, respectively. $K_{i,j}$ are ligand dissociation constants (values are shown below) and n denotes PFK number of protomers ($n = 4$). R and T represent the fraction of active (R) and inactive (T) conformation states of the enzyme PFK (18). c_α, c_δ, c_γ and c_β represent the non-exclusive binding coefficients of PFK defined as K_R/K_T for both substrates (F6P and ATP) and both allosteric effectors (ADP and PEP), respectively. L is the allosteric equilibrium coefficient of PFK and since $K_{R(A)} \neq K_{T(A)}$ and $K_{R(I)} \neq K_{T(I)}$, L is calculated according to Eq. [8], being $L_o = 4 \times 10^6$ (the allosteric constant in absence of any allosteric effector). Values of dissociation constants used in the model are (expressed in mM): $K_{1PEP} = 0.11$; $K_{2R(F6P)} = 1.25 \times 10^{-3}$; $K_{2T(F6P)} = 25$; $K_{2R(ATP)} = 6 \times 10^{-3}$; $K_{2T(ATP)} = 6 \times 10^{-3}$; $K_{2R(ADP)} = 2.5 \times 10^{-3}$; $K_{2T(ADP)} = 1.3$; $K_{2R(PEP)} = 750$; $K_{2T(PEP)} = 0.75$; $K_{3A1} = 0.31$; $K_{3B1} = 0.26$; $K_{3F1} = 0.19$.

In the model was assumed: i) negligible the extraglycolytic ATP consumption rate (6, 27), ii) constant intracellular concentrations of FDP (5 mM), Mg^{2+} (1 mM) and K^+ (100 mM) (6, 21, 27, 36, 37), and iii) the accumulation of pyruvate (PYR, depicted in Fig. 1) linked to a fast kinetics that removes PYR away from the system (not shown). Incidentally, PYR, does not affect the kinetic of the enzymes involved in the model.

Addition of Eqs. [1] and [4] leads to $d\text{ADP}/dt = -d\text{ATP}/dt$, therefore [ATP] + [ADP] = C_1 and since C_1 is constant (the model was studied with $C_1 = 3$ mM) the systems reduces to a three independent variables, ADP, PEP and F6P.

The analysis of Eqs. [1], [2], and [3] at steady state shows that:

$$v_2 = v_3,\ v_1 = v_2, \text{ and } 2v_2 = v_1 + v_3.$$

With these relationships and the corresponding functions associated with each v_i (Eqs. [5]–[10]) two fundamental expression were drawn and used for the analysis of the concentration of F6P and PEP at the steady state:

$$\sigma_1 \cdot \phi_1 = \sigma_3 \cdot \phi_3 \quad [11]$$

and

$$\sigma_1 \cdot \phi_1 = \sigma_2 \cdot \phi_2. \quad [12]$$

Whereas Eq. [11] has PEP and ADP as the independent variables, Eq. [12] is ATP, ADP, F6P and PEP dependent (see Eqs. [5]–[10]). These convenient relationships among parameters and variables allow evaluating the influence of different parameters on the steady state concentrations of ADP, PEP and F6P. From the pair of Eqs. [11] and [12] we can see that if only ADP (hence ATP) or any other variable (e.g., PEP or F6P) is considered constant the system would admit multiple steady state values for the rest of the variables. For this reason, in order to simplify the mathematical treatment, two variables at the time were considered constant. The characterization of the system at different steady states exceeds the scope of this communication and will be analyzed elsewhere.

The stability of linearized pair of Eqs. [1]–[2], [1]–[3], and [2]–[3] (with PEP, F6P or ADP constant, respectively) close to steady states was studied by analyzing their eigenvalues (38–40). Numerical and eigenvalue analyses were carried out by using Mathcad (ver.3.1) from MathSoft, and integration of differential equations was performed with DIFFEQ software (ver. 2.0) from MicroMath Inc.

RESULTS

Since ATP can be calculated from ADP and C_1 (3 mM) the study was conducted to investigate the influence of ADP, PEP and F6P on the dynamic behavior of the system described by Eqs. [1]–[3]. Figure 2a shows the temporal evolution of ADP, F6P and PEP when they are left to freely evolve. However, when ADP is considered constant, oscillations are suppressed for

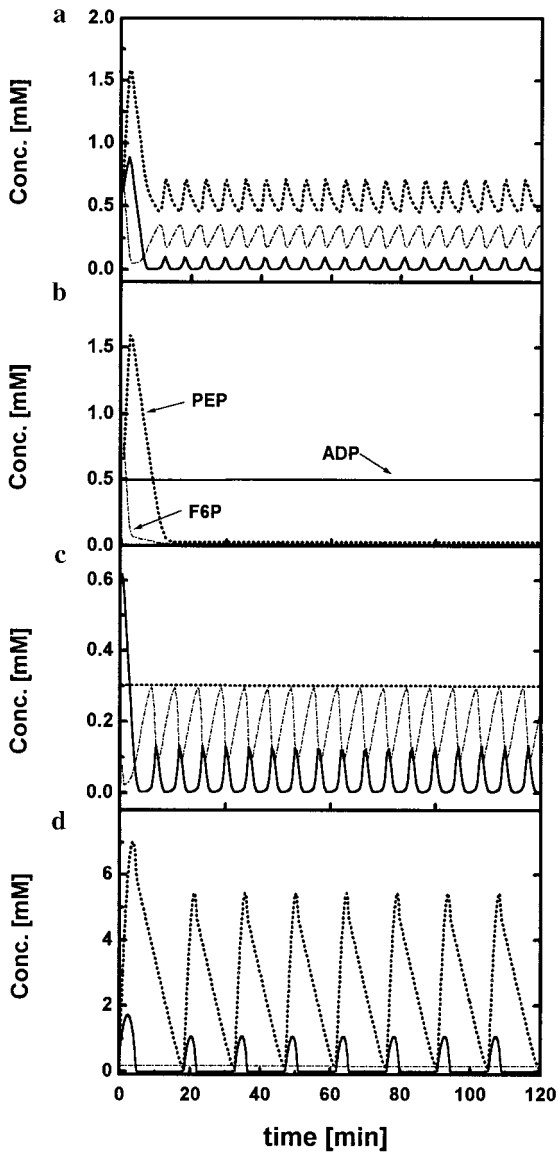

FIG. 2. Temporal evolution of ADP, F6P and PEP when none or one variable at the time is considered constant. (a) Evolution of the three variables when ADP, F6P and PEP are left to freely evolve; (b) evolution of F6P and PEP when ADP = 0.5 mM; (c) evolution of ADP and F6P when PEP = 0.3 mM, and (d) ADP and PEP evolution when F6P = 0.2 mM. Other parameters of the model are: σ_1 = 0.5 mM/min, σ_2 = 3.0 mM/min, σ_3 = 2.0 mM/min and C_1 = ATP + ADP = 3 mM. Lines: solid, ADP; dot, PEP; dot–dash, F6P.

any value of the other parameters (Fig. 2b). In contrast, when F6P or PEP is considered constant, and ADP evolves with the other variable according to the pair of Eqs. [1] and [2] or [1] and [3], the model regains the oscillatory behavior (Figs. 2c and 2d). Evaluation of the influence of the initial concentration of ADP reveals that the system always generates oscillations within the range of $10^{-4} <$ ADP < 2 mM, provided that ADP is not constant and regardless whether PEP or F6P are considered constant. The incorporation of the non-glycolytic ATP consumption rate into Eqs. [1] and [4] did not change the profiles.

When the concentration ADP is considered constant, the model is described by the pair of Eqs. [2] and [3]. With this constrain, analysis of Eqs. [11] and [12] reveals that there are two steady state points, one stable-node at (0, 0) independent to all parameters of the model (trivial solution), and the other, a saddle-point located in this case at (1.18, 0.57) but whose exact position depends not only on ADP but on σ_1, σ_2, σ_3 as well. Figure 3a shows the PEP–F6P phase portrait corresponding to a saddle point where trajectories of PEP and F6P associated to unstable and stable manifolds are strongly influenced by initial conditions and the parameters above mentioned. The stable manifold of the saddle-point defines a separatrix that divides the space PEP–F6P in an attracting basin that contains the stable-node at (0, 0) and a repellent basin where the system is always unstable. Consequently, if PEP and F6P concentrations lay near the region influenced by stable manifold branches, the system would show a stable or quasi-stable behavior with PEP and F6P trajectories approaching to the unstable steady state (saddle point). However, for perturbations of PEP or F6P as small as 0.05 mM, the system would change to a typical unstable behavior, inducing the complete exhaustion (when shifting toward the attracting basin), or the uncontrolled accumulation (when shifting toward the repellent basin) of PEP and F6P (Fig. 3a). Analysis of the stability of the linearized system close to a steady state reveals that the system fluctuates between a critically damped and an unstable dynamical behavior depending on initial conditions and values of parameters (results not shown).

When the concentration of PEP is considered constant, the pair of equations [1], [2] describe the model. Under steady state conditions the system has an unique real steady state point located at (0.248, 0.025) which is the node of the limit cycle depicted in Fig. 3b. This limit cycle is stable and spins counterclockwise with a frequency and amplitude that depend on the values of PEP and the other parameters of the model. In this case, whereas trajectories that lay outside of the cycle approach to the cycle stabilizing the system, points laying within the limit cycle spiral out the unstable node (steady state point) until their trajectories reach the limit cycle. Numerical analysis revealed that such oscillatory behavior extends from $0.04 <$ PEP $<$ 10 mM and beyond this range the unstable node becomes a stable node stabilizing the system at the corresponding steady state points (not shown).

When the concentration of F6P is considered constant, Eqs. [1] and [3] describe the model. Analysis of the system at a steady sate reveals that under these conditions there is a single real steady state point located within a limit cycle (0.257, 0.031). Figure 3c shows the PEP-ADP phase portrait diagram that cor-

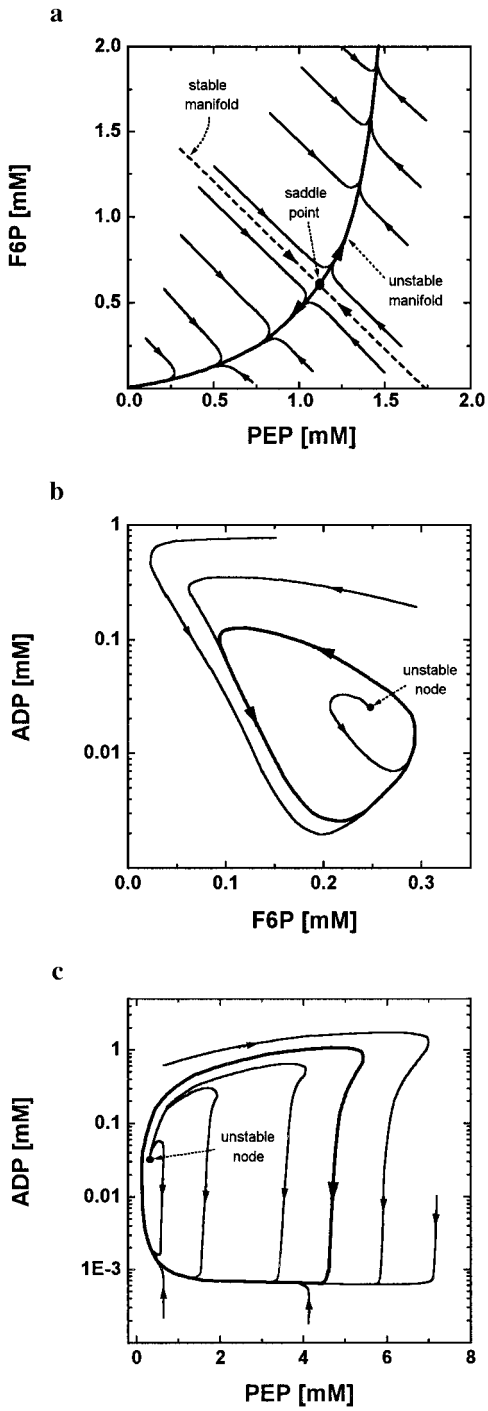

FIG. 3. Dynamic maps of the model depicted in Fig. 1 evaluated under different conditions. (a) PEP-F6P phase portrait of the model described by the pair of equations [2], [3] when ADP = 0.5 mM, σ_1 = 0.9 mM/min, σ_2 = 0.865 mM/min and σ_3 = 0.92 mM/min. Stable-node and saddle-point are located at (0, 0) and (1.18, 0.57), respectively. (b) F6P - ADP phase portrait described by Eqs. [1] and [2], when PEP = 0.3 mM, σ_1 = 0.5 mM/min, σ_2 = 3.0 mM/min, and σ_3 = 2.0 mM/min. Unstable node is located at (0.248, 0.025). (c) PEP–ADP phase portrait of the model described by Eqs. [1] and [3], when F6P = 0.2 mM, σ_1 = 0.5 mM/min, σ_2 = 3.0 mM/min and σ_3 = 2.0 mM/min. Unstable node is located at (0.257, 0.031). The rest of parameters as indicated under Model Description.

responds to a stable limit cycle that spins clockwise and whose outer trajectories sink to the cycle and inner trajectories escape out from the unstable node (steady state point) toward the limit cycle. Numerical analysis of the system depicted in Fig. 3c shows that the oscillatory behavior extends through a wide range of values of F6P concentration ($0.1 < F6P < 10$ mM) and beyond this range the dynamics of the systems switches from stable limit cycle to a stable node whose trajectories sink to the steady state point (not shown).

CONCLUSIONS

Although the model predicts oscillations during glucose consumption as was earlier suggested by Malkova *et al.* (41), this type of behavior has not yet been experimentally observed. However, that may be due to the experimental approach used to evaluate the concentration of those intracellular metabolites. Since oscillation periods are in the order of few minutes (Fig. 2) and intracellular concentrations determined by ^{31}P MNR experiments demand the accumulation of many FIDs (free induction decays) for 15–25 min (24–27), fluctuations of the concentration of metabolites around the steady state value would be undetectable. In fact, intracellular concentration of ADP, PEP, or F6P reported in the literature represent average values (27, 36, 37). Hence, the existence of an oscillatory behavior during glucose consumption cannot be completely ruled out.

The model presented in this paper shows that the system can display contrasting dynamic behavior depending on whether ADP, PEP or F6P are considered constant at a steady state. Such considerations become critical at the time of evaluating the intracellular concentration of these intermediate metabolites when a pseudo-steady state is assumed. From the literature (24–27) we can see that authors consider equally valid to assume anyone or all of these metabolites constant at a steady state. Nevertheless, if the concentration of ADP is constant at a steady state, the model predicts that the system would be considerably unstable (Fig. 3a) regardless the concentration of PEP and F6P. Since this metabolic scenario has not been observed in resting or active growing cells, we can conclude, therefore, that this situation is rather unlikely to occur in the cells. On the contrary, dynamics like those shown in Figs. 3b and 3c are more likely to occur, because the interaction among variables and parameters generates a very stable dynamic structure (e.g., limit cycles) that can damp almost any discrete perturbation. In the case depicted in Fig. 3c, trajectories of ADP and PEP pass through a wide range of concentrations, suggesting that ADP and PEP can act as activators and inhibitors of the system (see Fig. 1) while the rest of the intermediate metabolites of the glycolytic pathway may remain constant at a steady state. In conclusion, these results

show that ADP (and ATP) exerts a major influence on the dynamic behavior of the pathway.

Moreover, a detailed analysis of the enzymatic kinetic expressions used, suggests that ADP may have a stronger influence than ATP on the dynamic regulation of the system. The latter can be explained by analyzing the role of ADP on the regulation of the enzymes PFK and PK, both flux controlling enzymes in the pathway (4, 31). Whereas ADP exerts simultaneously a heterotropic feed-back-activation effect on the PFK (18, 19) and a homotropic cooperative effect on PK (20, 21), ATP does not.

Results obtained with this model suggest that although the concentration of PEP or F6P can eventually be constant at a given steady state (or pseudo-steady state), ADP (or ATP) should not. We may speculate that during cell growth the control of the steady state concentration of a particular metabolite could be temporarily regulated at different levels according to the physiological state or the phase of the cell cycle. In this way, the concentration (or flux) of ADP, PEP or F6P could be controlled by switching from one dynamic mode to another in response to intracellular or extracellular signals as was suggested earlier (6, 10). This complex regulatory scheme would further expand the regulatory capacity of bacteria adding flexibility and sensitivity to the their own genetic regulatory mechanisms.

ACKNOWLEDGMENTS

This work was partially supported by a grant from Fundación Antorchas, Argentina. J.C.D.R. is a Research Fellow of the Alexander von Humboldt Foundation and a researcher of CONICET.

REFERENCES

1. Higgins, J. (1967) *Ind. Eng. Chem.* **59,** 18–62.
2. Sel'kov, E. E. (1968) *Eur. J. Biochem.* **4,** 79–85.
3. Reich, J. G., and Sel'kov, E. E. (1974) *FEBS Lett.* **40,** 119–127.
4. Savageau, M. A. (1976) *in* Biochemical System Analysis. A Study of Function and Design in Molecular Biology, Addison-Wesley, London.
5. Markus, M., Kuschmitz, D., and Hess, B. (1984) *FEBS Lett.* **172,** 235–238.
6. Markus, M., and Hess, B. (1984) *Proc. Natl. Acad. Sci. USA* **81,** 4394–4398.
7. Markus, M., Kuschmitz, D., and Hess, B. (1985) *Biophys. Chem.* **22,** 95–105.
8. Higgins, J. (1965) *in* Control of Energy Metabolism (Chance, B., Estabrook, R. W., and Williams, G. R., Eds.), pp. 13–46. Academic Press, New York.
9. Goldbeter, A., and Nicolis, G. (1976) *Progr. Theor. Biol.* **4,** 65–160.
10. Decroly, O., and Goldbeter, A. (1982) *Proc. Natl. Acad. Sci. USA* **79,** 6917–6921.
11. Decroly, O., and Goldbeter, A. (1987) *J. Theor. Biol.* **124,** 219–250.
12. Goldbeter, A, Decroly, O., Li, Y. X., Martiel, J. L., and Moran, F. (1988) *Biophys. Chem.* **29,** 211–217.
13. Holms, W. H. (1986) *Curr. Top. Cell. Regul.* **28,** 69–105.
14. Postma, P. (1992) *in* Encyclopedia of Microbiology (Lederberg, J., Ed.), Vol. 3, pp. 339–349. Academic Press, New York.
15. Liao, J. C., Hou, Sh-Y., and Chao, Y-P. (1996) *Biotech. Bioeng.* **52,** 129–140.
16. Waygood, E. B., Meadow, N. D., and Roseman, S. (1979) *Anal. Biochem.* **95,** 293–304.
17. Saier, M. H., Jr., and Fagan, M. J. (1992) *in* Encyclopedia of Microbiology (Lederberg, J., Ed.), Vol. 1, pp. 431–442. Academic Press, New York.
18. Blangy, D., Buc, H., and Monod, J. (1968) *J. Mol. Biol.* **31,** 13–35.
19. Diaz Ricci, J. C. (1996) *J. Theor. Biol.* **178,** 145–150.
20. Markus, M., Plesser, Th., Boiteux, A., Hess, B., and Malcovati, M. (1980) *Biochem. J.* **189,** 421–433.
21. Boiteux, A., Markus, M., Plesser, Th., and Hess, B. (1983) *Biochem. J.* **211,** 631–640.
22. Heinrich, R., and Schuster, S. (1996) *in* The Regulation of Cellular Systems (Chapman and Hall, Eds.), pp. 55–59. International Thomson Publishing, New York.
23. Chen, R., and Bailey, J. E. (1993) *Biotechnol. Bioeng.* **42,** 215–221.
24. Ugurbil, K., Rottenberg, H., Glynn, P., and Schulman, R. P. (1978) *Proc. Natl. Acad. Sci. USA* **75,** 2244–2248.
25. Ugurbil, K., Rottenberg, H., Glynn, P., and Schulman, R. P. (1982) *Biochemistry* **21,** 1068–1075.
26. Axe, D. D., and Bailey, J. E. (1987) *Biotechnol. Lett.* **9,** 83–88.
27. Diaz Ricci, J. C., Hitzmann, B., and Bailey, J. E. (1991) *Biotechnol. Prog.* **7,** 305–310.
28. Moran, F., and Goldbeter, A. (1984) *Biophys. Chem.* **20,** 149–156.
29. Gottschalk, G. (1986) Bacterial Metabolism, 2nd ed. Springer-Verlag, New York.
30. Sanwal, B. D. (1970) *Bacteriol. Rev.* **34,** 20–39.
31. Kacser, H., and Burns, J. A. (1973) *Symp. Soc. Exp. Biol.* **27,** 65–104.
32. Hofmann, E. (1976) *Rev. Physiol. Biochem. Pharmacol.* **75,** 1–68.
33. Heinrich, R., Rapoport, S. M., and Rapoport T. A. (1977) *Prog. Biophys. Mol. Biol.* **32,** 1–82.
34. Gonzalez, J. E., and Peterkofsky, A. (1977) *J. Supramol. Struct.* **6,** 495–502.
35. Monod, J., Wyman, J., and Changeaux, J. P. (1965) *J. Mol. Biol.* **12,** 88–118.
36. Morikawa, M., Izui, K., Taguchi, M., and Katsuki, H. (1980) *J. Biochem.* **87,** 441–449.
37. Neuhard, J., and Nygaard, P. (1987) *in Escherichia coli* and *Salmonella typhimurium:* Cellular and Molecular Biology. Purines and Pyrimidines (Neidhardt, F. C., Ed.), Vol. 1, Chap. 29, p. 447. ASM Washington, DC.
38. Segel, L. A. (1980) *in* Mathematical Models in Molecular and Cellular Biology, pp. 607–744. Cambridge University Press, Cambridge.
39. Thompson, J. M. T., and Stewart, H. B. (1988) *in* Nonlinear Dynamics and Chaos, pp. 15–64. Wiley, New York.
40. Seydel, R. (1988) *in* From Equilibrium to Chaos. Practical Bifurcation and Stability Analysis, pp.15 –64. Elsevier Science Publishers Ltd., New York.
41. Malkova, I. A., Popova, S. V., and Sel'kov, Y. Y. (1980) *Biofizika* **25,** 503–507.